Reliability Engineering and System Safety 175 (2018) 119–127

Contents lists available at ScienceDirect

Reliability Engineering and System Safety

journal homepage: www.elsevier.com/locate/ress

Reliability analysis of phased mission system with non-exponential and partially repairable components

Xiang-Yu Li[a,b], Hong-Zhong Huang[b,*], Yan-Feng Li[b]

[a] School of Mechanical and Electrical Engineering, University of Electronic Science and Technology of China, No. 2006, Xiyuan Avenue, West Hi-Tech Zone, Chengdu, Sichuan 611731, PR China

[b] Center for System Reliability and Safety, University of Electronic Science and Technology of China, No. 2006, Xiyuan Avenue, West Hi-Tech Zone, Chengdu, Sichuan 611731, PR China

A R T I C L E I N F O

Keywords:
Phased mission system
Semi-Markov process
Approximation algorithm
AOCS in satellite

A B S T R A C T

Phased mission systems (PMSs) have wide applications in engineering practices, especially in aerospace industry such as man-made satellite and spacecraft. To achieve high reliability in a PMS, certain critical parts in the system are designed to have a redundant architecture, such as cold standby (structural or functional). State-space models such as Markov processes have been widely used in previous studies to evaluate the reliabilities of these systems. But in practice, many real systems consist of mechanical components or mechatronics whose lifetime follow non-exponential distributions like the Weibull distribution. In this type of system, the Markov process is not capable of modeling the system behavior. In this paper, the SMP (Semi-Markov Process) is applied to solve the problem that the components' lifetime in dynamic systems follows non-exponential distributions. An approximation algorithm for the SMP is proposed to assess the reliability of the PMSs consisting of non-exponential components. Furthermore, the accuracy and calculation efficiency of the approximation algorithm are explored. At last, the reliability assessment of a complex multi-phased altitude and orbit control system (AOCS) in a man-made satellite is presented to illustrate the method.

1. Introduction

A phased mission system (PMS) is defined as a system subject to multiple, consecutive, non-overlapping operation phases [1]. During each phase, a PMS needs to accomplish a specified task. In these phases, the system may be subject to different working conditions and environmental stresses, as well as different performance requirements. Take a manned spacecraft as an example—one flight of the spacecraft involves lifting off, on-orbit operation, leaving orbit, and landing phases. In each phase, the spacecraft needs to accomplish a specific mission and work under specific working conditions (lifting off phase and landing phases in endo-atmosphere, on-orbit and leave orbit in the outer space). So in different phases, the system configurations, and the components' failure rates and even failure criteria could be vastly different. So distinct models for different phases are necessary to model and analyze the PMS accurately. To analyze the reliability throughout the whole lifetime of the PMS, the s-dependency across the multiple phases should be considered. For instance, in a non-repairable PMS, once a component fails in an early phase, it will remain in a down state in subsequent phases [2,3]. The consideration of such dependency raises grand challenges to the existing single-phase reliability modeling method [4].

The reliability of a PMS is defined as the probability that the system achieves all the mission objectives successfully in all phases. Over the past decades, researchers have proposed a number of PMS reliability analysis models. These modeling models could be divided into two major categories:

(1) State space models based on stochastic processes [5,6], such as continuous-time Markov chain (CTMC) based models and Petri-net based models. The main idea of the CTMC based modeling method is to construct a Markov chain for each phase to represent the system behavior of the PMS. The dependency among components like cold standby can be modeled by a Markov model. However, the Markov model may suffer from the state explosion problem when the number of the system states grows large.
(2) Combinatorial models [1,7], such as BDD and MDD based models. The fundamental assumption of the combinatorial models is that all the components are independent of each other, which means there is no dependency existing within one phase. But the dependency among phases still need to be accounted for. The key to adopt the BDD to a multi-phase system is the phase algebra. Detailed information about the phase algebra can be found in [2].

* Corresponding author.
E-mail address: hzhuang@uestc.edu.cn (H.-Z. Huang).

https://doi.org/10.1016/j.ress.2018.03.008
Received 29 October 2016; Received in revised form 7 January 2018; Accepted 3 March 2018
Available online 6 March 2018
0951-8320/

Acronyms

AOCS	altitude and orbit control system
BDD	binary decision diagram
CDF	cumulative distribution function
CSP	cold spare
CTMC	continuous time Markov chains
MCS	Monte Carlo Simulation
MDD	multi-valued decision diagram
MFT	modularized fault tree
PDO	phase-dependent operation
PMS	phased mission system
PMS–BDD	a BDD-based PMS approach
SMP	semi-Markov process

Notation

$\boldsymbol{Q}(t)$	the kernel matrix of SMP at time t
$\boldsymbol{\theta}(t)$	the transition probability matrix of SMP at time t
$Q_{i,j}(t)$	the state transition probability from state i to state j at time interval [0, t]
$\theta_{i,j}(t)$	the probability that SMP starts in state i at $t = 0$ and ends in state j at time t
K	the amount of states of the SMP
$F_i(t)$	the CDF of lifetime of component i
$G_i(t)$	the CDF of repair time of component i
$\alpha,\ \beta$	shape parameter and scale parameter of the Weibull distribution
L	the amount of segments
δ	the discretization interval length
$M_{i,j}$	the ith module in phase j
T_i	the phase duration of phase i
$F_{M_i}(t)$	the CDF of module i at time t
$F_{M_{i,j}}(t)$	the CDF of module i at time t of phase j
$w,\ f,\ s$	representing state of the components in working, failure and standby separately.
R_{sys}	system reliability
Si_{Mj}	state i of module j
T_w	the whole lifetime of the phased AOCS

Though the above two types of models can be used to address the challenges in PMS reliability modeling and assessment, they both have some serious limitations. The state space models cannot be used in large-scale systems due to the exponential growth of the state number. On the other hand, combinatorial models can deal with the large-scale system problems but cannot effectively analyze the dynamic behaviors of complex systems. To make use of the advantages of these two methods, a modularization method [3] combining PMS–BDD and Markov process has been proposed. Based on the fault tree modularized method, all components can be classified into two categories: independent static modules and dynamic modules. The static modules are assessed efficiently using PMS–BDD method, and the dynamic modules are assessed based on the Markov method. This hybrid approach possesses the advantages of both methods, namely computational efficiency and effective dynamic behavior representation.

As is well known, many real-world systems, particularly those aerospace equipment like manmade satellite, are designed with cold-standby redundancy for achieving fault tolerance and high reliability [8–12]. On the other hand, due to the weight restriction and travelling in the outer space, only a few components in the satellite can be repaired by limited maintenance resources. To evaluate reliability of this type of system, the use of a state space model is necessary. In a traditional Markov chain, the sojourn time among states follows the exponential distribution [13–16]. But many real-world systems like the satellite consist of mechanical or electromechanical components whose lifetime and repair time are very likely to follow non-exponential distributions such as Weibull distribution. With the non-exponential lifetime distributions [17], the system cannot be modeled by the traditional Markov process. However, semi-Markov process [18], belonging to non-Markovain family, can deal with the non-exponential transition times [18–20]. Therefore, the semi-Markov process (SMP), in conjunction with the modularization method and PMS–BDD models, is adopted in this paper to evaluate the reliability of the complex PMS.

The main contribution of this paper is the development of a semi-Markov based model for reliability evaluation of complex phased mission systems consisting of partially repairable non-exponential components. Meanwhile, through combining the SMP and the modularization method, the system reliability can be assessed with fewer states than only using the SMP. To mitigate the calculation complexity and improve the computational efficiency, an approximation method (the Trapezoidal integration rule) is used to compute the complex integrals. The accuracy and calculation efficiency of this approximation method are carefully examined.

The rest of this paper is organized as follows. Section 2 introduces the basics of semi-Markov process (SMP) and the approximation method. In Section 3, the accuracy and the calculation efficiency of the approximation method are explored in detail. Section 4 presents in detail a practical system, the altitude and orbit control system of a satellite, and its multi-phased and dynamic behaviors. Furthermore, the modular method is applied to simplify the system FT model. In Section 5, the SMP as well as the approximation method is applied to evaluate the reliability indices of dynamic modules and the mini-component method is applied to evaluate the reliability indices of static modules. By combining the reliability indices of dynamic modules and static modules, the reliability of the multi-phased AOCS can be assessed by the PMS–BDD model. A conclusion of this paper along with a summary of our future works is presented in Section 6.

2. Approximation method for SMP

2.1. Basic conception of semi-Markov process

Although CTMC possesses many desirable characteristics and is widely used in reliability modeling, the transition time needs to follow the exponential distribution, which limits its applications in reality, especially in systems consisting of non-exponential components. In a semi-Markov process (SMP), the state transition time can be any kinds of distributions which is critical to solving this type of problem. SMP is a generalization of the classical Markov chains as it accommodates arbitrary sojourn time distributions. Generally, SMP does not have the Markov property, except for transition time points. These time points are the Markov regeneration epochs, and the SMP only changes the states at these epochs. That is why it is called a semi-Markov process [20].

To define the transient behaviors of a SMP, the initial system state probability vector $\boldsymbol{P}(t)$ at time $t = 0$ and the kernel matrix $\boldsymbol{Q}(t)$ in which element $Q_{i,j}(t)$ denotes the probability that the SMP transitions from state i to state j during the time interval [0, t]. The kernel matrix $\boldsymbol{Q}(t)$ can be obtained by the cumulative distribution function (CDF) of sojourn time between states and the competition behaviors among transitions.

The main task in using the SMP for reliability assessment is to evaluate the system state probabilities at any time t. Let $\boldsymbol{\theta}(t)$ represent the transition probability matrix in which $\theta_{i,j}(t),\ i,j = \{1,2,\cdots,K\}$ represents the probability that the process start from state i to state j at time interval [0, t]. According to [18], the state probabilities $\theta_{i,j}(t),\ i,j = \{1,2,\cdots,K\}$ can be derived by solve the integrals given below,

$$\theta_{i,j}(t) = \sigma_{i,j}\left(1 - F_i(t)\right) + \sum_{k=1}^{K}\int_0^t q_{i,k}(\tau)\theta_{k,j}(t-\tau)d\tau \tag{1}$$

where, $q_{i,k}(t) = \frac{dQ_{i,k}(t)}{dt}$, $F_i(t) = \sum_{j=1}^{K} Q_{i,j}(t)$, $\sigma_{i,j} = \begin{cases}1, & if \quad i = j\\ 0, & if \quad i \neq j\end{cases}$

It can be observed that the first part of Eq. (1) is the probability that the system stays in state i at time interval [0, t] and the second part of

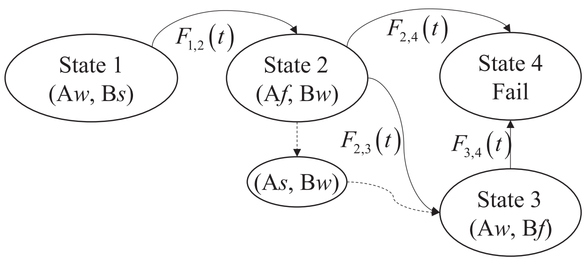

Fig. 1. State transition graph of the numerical example.

the equation represents the probability that system transits from state i to state j at time interval [0, t].

By integrating the calculated $\theta_{i,j}(t)$ and the given initial system state probabilities, the system state probabilities at time t can be assessed. With the system state probabilities at any time t, all the system reliability indices can be evaluated easily.

2.2. Approximation method for semi-Markov process

Although SMP can deal with the situation that state transition times follow non-exponential distributions, it is not widely used in reliability engineering. One important reason is that the integrals in Eq. (1) cannot be solved analytically under non-exponential distributions (e.g. Weibull distribution). In this paper, an approximation method based on Trapezoidal integral law is proposed to provide an approximate solution of the complex integrals in SMP. Trapezoidal integral law is a numerical method to compute the complex integral functions with approximate solutions.

To introduce the approximation method, a system with one working (A) and one cold standby (B) components is applied in this section. Component A can be repaired. Assume that component B will work immediately after the failure of Component A and the switchover time is negligible. $F_A(t)$ and $F_B(t)$ represent the CDFs of components' lifetime and $G_A(t)$ represent the CDF of the repair time of component A. $F_A(t)$, $F_B(t)$ and $G_A(t)$ follow the two parameter Weibull distributions ($F(t) = 1 - e^{-(t/\beta)^{\alpha}}$) with different parameters. The state transition graph is shown in Fig. 1 and only the state 4 is the failure state.

In Fig. 1, *w, s* and *f* respectively denotes a component staying at working, standby and failure states and $F_{i,j}(t)$ represent the CDF of the system transits from state i to state j. And the state transition behaviors can be described as,

- $S_1 \to S_2$: component A fails and the cold spare component B start to work;
- $S_2 \to S_3$: the repair of component A has completed before component B fails and component A starts to work after component B fails;
- $S_2 \to S_4$: the repair of component A has not completed before component B fails, and the system fails;
- $S_3 \to S_4$: component A fails again after repaired, and the system fails.

According to the definition of the semi-Markov process [18], the system state probabilities of this MSS can be calculated by the semi-Markov model by four steps as follows.

Step 1: Ascertain the structure of the kernel matrix $\boldsymbol{Q}(t)$ and transition probability $\theta(t)$ by the state-space diagram. According to the state transition behavior in Fig. 1, the kernel matrix $\boldsymbol{Q}(t)$ and state transition probability matrix $\theta(t)$ can be ascertained as,

$$\boldsymbol{Q}(t)=\begin{Bmatrix} 0 & Q_{1,2}(t) & 0 & 0 \\ 0 & 0 & Q_{2,3}(t) & Q_{2,4}(t) \\ 0 & 0 & 0 & Q_{3,4}(t) \\ 0 & 0 & 0 & 0 \end{Bmatrix}$$

$$\boldsymbol{\theta}(t)=\begin{Bmatrix} \theta_{1,1}(t) & \theta_{1,2}(t) & \theta_{1,3}(t) & \theta_{1,4}(t) \\ 0 & \theta_{2,2}(t) & \theta_{2,3}(t) & \theta_{2,4}(t) \\ 0 & 0 & \theta_{3,3}(t) & \theta_{3,4}(t) \\ 0 & 0 & 0 & \theta_{4,4}(t) \end{Bmatrix} \tag{2}$$

Step 2: Evaluate the kernel matrix $\boldsymbol{Q}(t)$. $Q_{i,j}(t)$ represents the probability that the system transits from state i to state j during time interval [0, t] with one step, like the one step transition probability in the Markov chain. For example, $Q_{2,3}(t)$ denotes the component B fails before the repair of component A is completed and $Q_{2,4}(t)$ denotes component B fails after the repair of component A has completed, and they can be computed as,

$$\begin{aligned} Q_{2,3}(t) &= \Pr\{(Ft_B \le t)\&(Rt_A < Ft_B)\} = \int_0^t G_A(u)dF_B(u) \\ Q_{2,4}(t) &= \Pr\{(Ft_B \le t)\&(Rt_A > Ft_B)\} = \int_0^t (1 - G_A(u))dF_B(u) \end{aligned} \tag{3}$$

where Ft and Rt represent the specific failure and repair time, respectively.

And the $q_{2,3}(t)$ and $q_{2,4}(t)$ *are,*

$$\begin{aligned} q_{2,3}(t) &= \frac{dQ_{2,3}(t)}{dt} = G_A(t)f_B(t) \\ q_{2,4}(t) &= \frac{dQ_{2,4}(t)}{dt} = (1 - G_A(t))f_B(t) \end{aligned} \tag{4}$$

The rest of the elements in $\boldsymbol{Q}(t)$ can be calculated according the state transition behaviors, shown as,

$$\boldsymbol{Q}(t)=\begin{Bmatrix} 0 & F_A(t) & 0 & 0 \\ 0 & 0 & \int_0^t G_A(u)dF_B(u) & \int_0^t (1 - G_A(u))dF_B(u) \\ 0 & 0 & 0 & F_A(t) \\ 0 & 0 & 0 & 0 \end{Bmatrix} \tag{5}$$

Step 3: Evaluate the state probability matrix $\theta(t)$ using Eq. (1) and the Trapezoidal integral law.

First, we can obtain the integral equations by Eq. (1) and the kernel matrix $\boldsymbol{Q}(t)$, shown as,

$$\begin{cases} \theta_{1,1}(t) = 1 - Q_{1,2}(t) & \theta_{2,2}(t) = 1 - Q_{2,3}(t) - Q_{2,4}(t) \\ \theta_{1,2}(t) = \int_0^t q_{1,2}(\tau)\theta_{2,2}(t-\tau)d\tau & \theta_{2,3}(t) = \int_0^t q_{2,3}(\tau)\theta_{3,3}(t-\tau)d\tau \\ \theta_{1,3}(t) = \int_0^t q_{1,2}(\tau)\theta_{2,3}(t-\tau)d\tau & \theta_{2,4}(t) = \int_0^t q_{2,3}(\tau)\theta_{3,4}(t-\tau)d\tau \\ \theta_{1,4}(t) = \int_0^t q_{1,2}(\tau)\theta_{2,4}(t-\tau)d\tau & \qquad + \int_0^t q_{2,4}(\tau)\theta_{4,4}(t-\tau)d\tau \\ \theta_{3,3}(t) = 1 - Q_{3,4}(t) & \theta_{3,4}(t) = \int_0^t q_{3,4}(\tau)\theta_{4,4}(t-\tau)d\tau \end{cases} \tag{6}$$

Second, the integrals in Eq. (6) are assessed by the two point trapezoidal rule [21], using $\theta_{1,2}(t)$ as an example, shown as follows,

$$\begin{aligned} \theta_{1,2}(t) &= \int_0^t q_{1,2}(\tau)\theta_{2,2}(t-\tau)d\tau \\ &\approx \sum_{k=1}^{L} \frac{1}{2}\left[q_{1,2}(\tau_k)\theta_{2,2}(t-\tau_k) + q_{1,2}(\tau_{k+1})\theta_{2,2}(t-\tau_{k+1})\right]\cdot(\tau_{k+1}-\tau_k) \end{aligned} \tag{7}$$

where [0, t] is divided into L equal segments of equal length and the discretization interval length is $\delta = t/L$ and τ_1=0, $\tau_{L+1} = t$.

Generally speaking, the smaller δ is, the more accurate result is. With Eq. (7), the integrals in Eq. (6) can be evaluated with an approximation solution.

Step 4: Based on the probability $\theta_{i,j}(t)$ at certain time t and the initial state vector $P(0)$, the system state probabilities at time t, $\boldsymbol{P}(t)$, can be evaluated as,

$$\boldsymbol{P}(t) = \boldsymbol{P}(0)\boldsymbol{\theta}(t) \tag{8}$$

With the system state probability $\boldsymbol{P}(t)$ at any time $t > 0$, all the reliability indices of this multi-state system can be computed easily.

Table 1
Parameters for the MSS in non-Markovian environment.

	$F_A(t)$	$F_B(t)$	$G_A(t)$
α	2	1.5	1.5
β	10	10	20

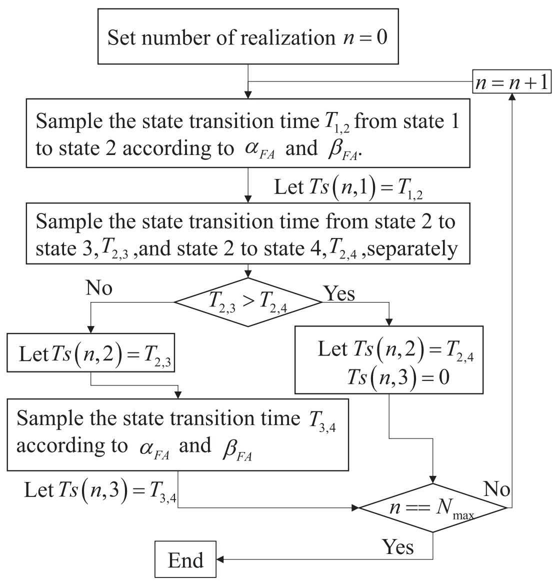

Fig. 2. The Monte Carlo simulation procedure for the numerical example.

3. Accuracy validation of the approximation method

In the previous section, an approximation method is proposed to assess the SMP and be able to provide an approximation solution [22,23]. In this section, the accuracy of the approximation method is studied by comparing the results on the example shown in Fig. 1 by the Monte Carlo simulation method and the approximation method. Furthermore, the calculation efficiency of the approximation method is also investigated.

The parameters of the Weibull distributions are shown in Table 1. α is the shape parameter and β is the scale parameter. The initial state probabilities are $\boldsymbol{P}(0)=(p_1(0)=1,\ p_2(0)=p_3(0)=p_4(0)=0)$.

With known transition time distributions and the approximate method shown in Section 2, the system reliability can be evaluated with the discretization interval length $\delta=0.1$. And the calculation time is only 0.22 s.

To demonstrate the accuracy of the result assessed by the approximation method. A Monte Carlo simulation (MCS) method is applied in this part. MCS is based on repeated sampling of realizations of system configurations. By statistically analyzing simulated data, the reliability indices, such as the system reliability, can be assessed. All the data simulated represent the seldom of failure, so with more realizations (more simulated failure data), the analysis result will be more accurate [22]. The simulation procedure for the numerical example is shown in Fig. 2.

In Fig. 2, $T_{i,j}$ represents the simulated time that the system transit from state *i* to state *j* and *Ts*(*j, i*) represent the recorded time that system stays in state *i* in the *j*th simulation. With the simulation procedure, the comparison of the system state probabilities by the approximation method and MC simulation (simulation amount $N_{\max}=2\times10^5$) method are shown in Fig. 3.

To show the calculation efficiency and accuracy of the approximation method, different amount of data are used to evaluate the reliability of the numerical example. First, $N_1(N_1=500)$ failure time data are generated by using the MCS method. The comparison between the approximation method and MC simulation method is shown in Fig. 4(a) with $N_1=500$ and the errors are obvious. As mentioned above, the result by the MCS method is more accurate with more data. So the amount of simulation data is increased to N_2=5×10^3, N_3=5×10^4, $N_4=5\times10^5$ and $N_5=5\times10^6$, respectively. With the simulation amount $N_2=5\times10^5$, the comparison is shown in Fig. 4(b) and the errors decrease obviously. The max errors and the mean errors of the system reliability under different data amount are shown in Table 2 as well.

As is well known, with the increase of the realization amount, the simulation result gets closer to the true value, and from Table 2, we can see that the max error and mean error between the two methods get smaller. The results illustrate that the approximation method can provide a relatively accurate solution. On the other hand, from the calculation times shown in Table 2, if we want to get a highly accurate solution by the MCS method, the calculation time will be much longer compared to the approximation method.

4. Multi-phased AOCS in manmade satellite

4.1. The AOCS in the manmade satellite

In this section, the altitude and orbit control system (AOCS), a critical subsystem of the manmade satellite, is introduced as a practical example to illustrate the reliability modeling process of phased mission system. The AOCS in a satellite is used to control and adjust the orbit and altitude in the whole lifetime.

The AOCS has three subsystems: the control subsystem (AOCC, altitude and orbit control computer), the sensor subsystem (including sun sensor, earth sensor, star track sensor and gyro assembly) and the actuator subsystem (thrusters and momentum wheels).

The AOCS can be regarded as feed-back system with three steps shown in Fig. 5. In the first step, the sensor subsystem acquires and collects the position and altitude data. In the second step, the position and altitude data is transited to and analyzed by the control subsystem. In the third step, according to the analyzed result, the control subsystem will send orders to the actuator system to adjust the position and altitude. Then comes next measurement and adjustment procedure. The repeating of this procedure keep the manned satellite in the right altitude and orbit in the whole lifetime.

According to different tasks to be completed in different phases, the whole lifetime of the AOCS can be divided into three phases—launching phase, orbit transfer phase and orbital operation phase. In each phase, the system will execute different tasks in conjunction with other subsystems in the satellite.

The control subsystem consists of two components, computer A and cold standby computer B. Computer A can be repaired by backup components. The sensor subsystems consists of four components: sun sensor (C), earth sensor (D), star track sensor (E) and gyro assembly (F). Only part of these sensors work in one specific phase. For example, the sun sensor and the earth sensor work in phase 1 and the earth sensor, the star track sensor and the gyro assembly work in phase 2. The actuator subsystem consists of two parts: thrusters and momentum wheels which will work as actuators in different phases. There are two types of thrusters: two 15 N thrusters in cold standby (H, I, used for slightly adjustment during orbit transfer) and one 620 N thruster (G, the major power source for orbit transfer and adjustment). The momentum wheels (J, K and L) are designed as a 2-out-of-3 system and they work in phase 3. The FT models for the 3 phases are shown in Fig. 6.

4.2. System modularization of the AOCS

From the description in last section, the FT models will be too complicated to solve if the state space model is directly used. To address this problem, a modularization method defined in [24] and used in [3] is applied to deal with the cold standby behaviors. A phase module of a multi-phased system must meet two conditions: (1) A module is a set of

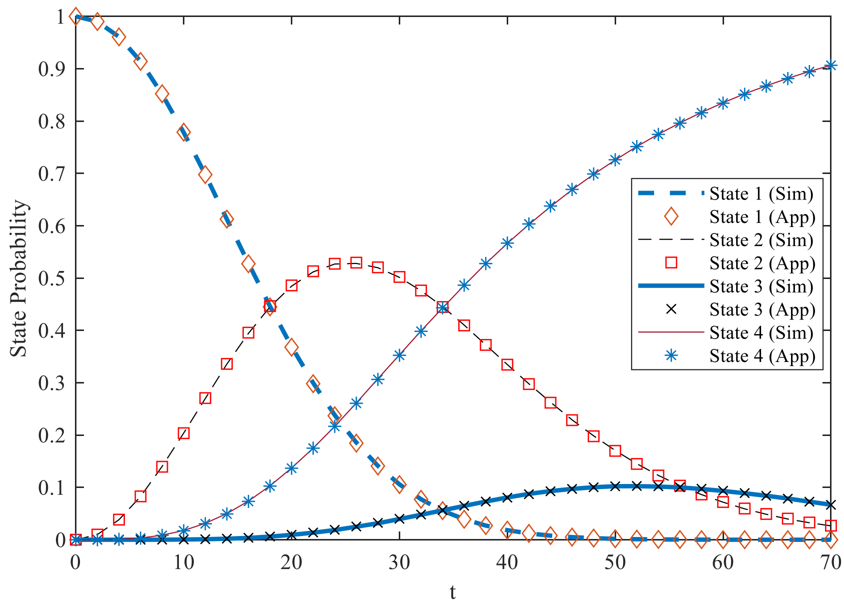

Fig. 3. State probabilities of the numerical example by approximation and simulation approaches.

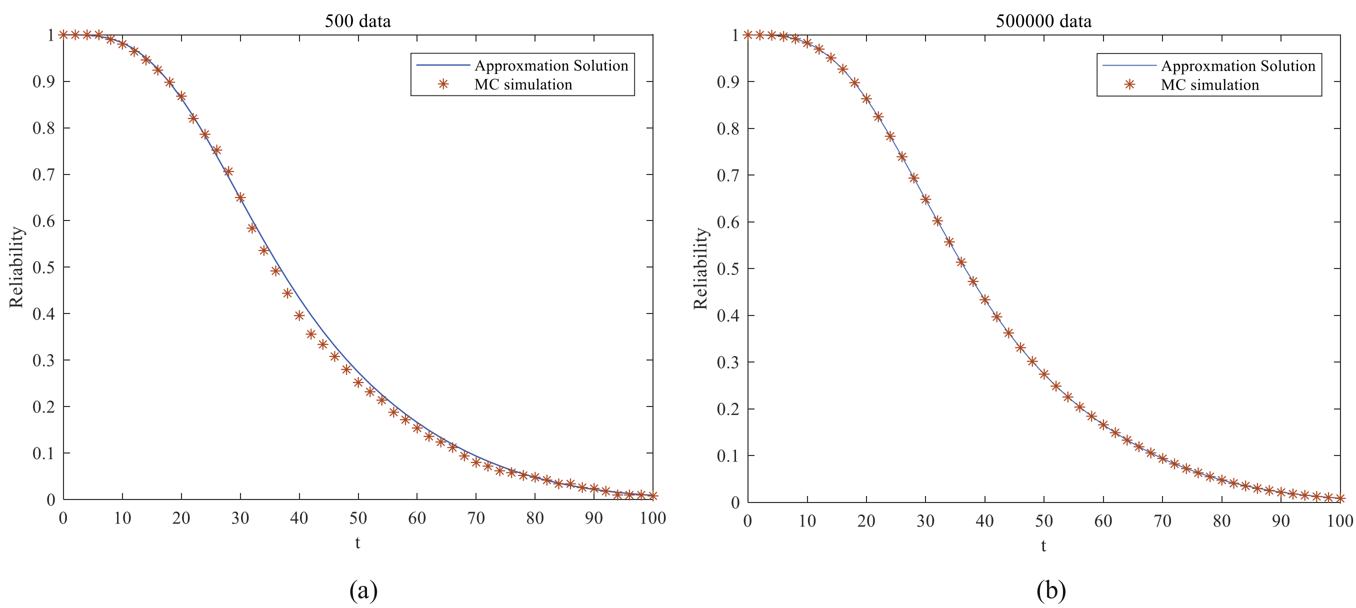

Fig. 4. The comparison between the MCS and approximation method under different data amount.

Table 2
The errors between the simulation method and approximation method.

Simulation data amount	5×10^2	5×10^3	5×10^4	5×10^5	5×10^6
Max error	4.96×10^{-2}	1.98×10^{-2}	4.37×10^{-3}	2.75×10^{-3}	4.49×10^{-4}
Mean error	1.10×10^{-2}	4.27×10^{-3}	1.04×10^{-3}	8.16×10^{-4}	2.66×10^{-4}
Calculation time(s)	0.69	5.37	60.59	773.44	6062.06

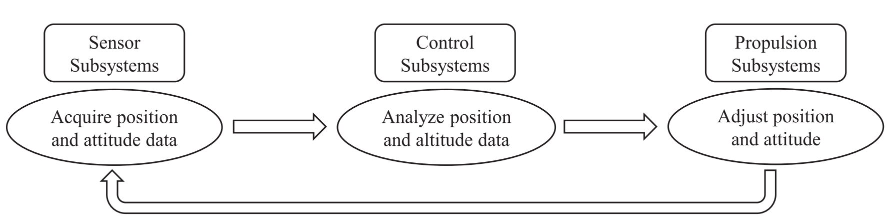

Fig. 5. The working process of AOCS of satellites.

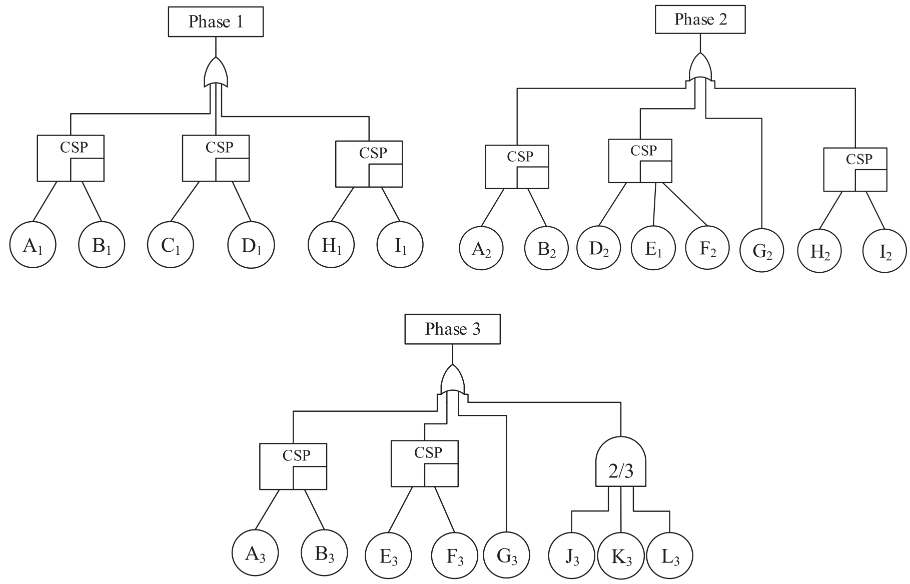

Fig. 6. The FT model for three phases of the AOCS.

basic events, which means a module must be a subset of all basic events; (2) For each phase, the basic events in the collection form an independent sub-tree in the fault tree [3]. In another word, different sub-trees in one phase should be independent on each other. After modularization, the modularized fault tree consists of the independent sub-trees (modules), and as a result, the complicated PMS can be assessed easily by the PMS–BDD method and module reliabilities.

Four steps are involved in the reliability assessment of the PMS by the modularization method and PMS–BDD method. These steps are detailed as follows.

Step 1: Divide the fault trees of the three phases into several independent subtrees by the modularization method [24]. According to their own characteristics, the subtrees (modules) can be divided into static modules and dynamic modules. A module is a static module if it contains only static logic gates (*and, or, k-out-of-n*). If there are dynamic logic gates, such as the cold spare, the module is a dynamic module [16].

Step 2: After modularization, the modules can be treated as the bottom events of the modularized fault trees (MFT). In the MFT, the modules are independent of each other.

Step 3: According to the characteristics of the modules, the reliability indices of dynamic and static modules can be assessed by SMP as well as the approximation method and the mini-component method, respectively.

Step 4: Integrating the results of Step 2 and Step 3, the system reliability can be assessed by using the PMS–BDD method.

There are twelve basic events $\{A, B, C, D, E, F, G, H, I, J, K, L\}$ in this PMS. All the components can be divided into several modules in the three phases. And the relationship between independent modules and basic events in three phases are shown as,

$$\pi_1=\{M_{1,1}=(A,B), M_{2,1}=(C,D), M_{4,1}=(H,I)\} \tag{9}$$

$$\pi_2=\{M_{1,2}=(A,B), M_{2,2}=(D,E,F), M_{3,2}=G, M_{4,2}=(H,I)\} \tag{10}$$

$$\pi_3=\{M_{1,3}=(A,B), M_{2,3}=(E,F), M_{3,3}=G, M_{5,3}=(J,K,L)\} \tag{11}$$

$\pi_i, i=1,2,3$ represents the set of components working in phase *i*. $M_{i,j}$ represents the *i*th module in phase *j*.

Because some modules (e.g., $M_{2,2}$) are not consistent across phases, the module across phases need to be formed. With the set theory, the modules across phases can be obtained and shown as [3],

$$\{M_1=(A,B), M_2=(C,D,E,F), M_3=G, M_4=(H,I), M5=\{J,K,L\}\} \tag{12}$$

After the system modularization, all the basic events of the original FT model are divided into five independent modules. All the modules can be treated as basic events in the MFT model, shown as Fig. 7.

5. Reliability assessment of the AOCS

In this section, the evalution procedure of the AOCS reliability by the approximation method is shown in detail. In the last section, the FT models of the AOCS has been simplified into the MFT model. The SMP and the mini-components method are used to evaluate the dynamic and static module reliabilities in each phase separately. Since all the modules in the MFT are mutually independent, the system reliability can be evaluated based on the module reliabilities by the PMS–BDD method.

At first, all the modules are divided into three categories: From the descriptions in Section 4.1, modules 3 and 5 are static modules. The system structure of module 1 and module 4 do not change in different phases. And the system structure of module 2 changes in different phases, which needs specially designed methods to be dealt with. All the components are characterized by Weibull distributions. The parameters of all the components are listed in Table 3. The phase durations are $T_1=48, T_2=252$ and $T_3=5000$, respectively.

5.1. Module reliability

5.1.1. The static module

In this section, the mini-component method is used to evaluate the reliability of the static module. In the MFT, module 3 and module 5 are static modules. Here we use the module 5 as an example. Module 5 consists of three components, and system operation requires at least two components be operational. The failure probability of a k-out-of-n system such as module 5 (2-out-of-3 system) in a single phase can be expressed as [25],

$$p_{M_5}(t)=\sum_{i=k}^{n} C_n^i\left(1-F_{M5}(t)\right)^i\left(F_{M5}(t)\right)^{n-i},\quad F_{M5}(t)=1-e^{-(t/\beta_{M5})^{\alpha_{M5}}} \tag{13}$$

where $F_{M5}(t)$ represents the CDF of each component in module 5.

To deal with the dependency of the static modules among phases, a set of mini-components is used to replace the unit in one specific phase. Using module 5 as an example, the RBD and FT of this method [2] are shown in Fig. 8.

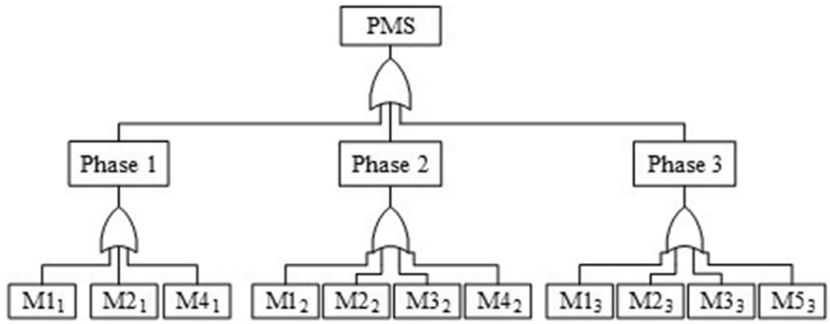

Fig. 7. The modularized FT (MFT) model.

Table 3
Parameters for the AOCS.

Components	Phase 1		Phase 2		Phase 3	
	α_1	β_1	α_2	β_2	α_3	β_3
A\B	2	500	2	500	1.5	1.5×10^4
AG	2	900	2	900	2	900
C\D\E\F	1.5	400	1.5	600	3	1×10^4
EG	1.8	600	1.8	600	1.8	600
G	1.5	1000	1.5	1500	2	3×10^4
H\I	2	600	1.8	300	1.5	1×10^4
J\K\L	1.5	1500	2.5	1500	2.5	3.2×10^4

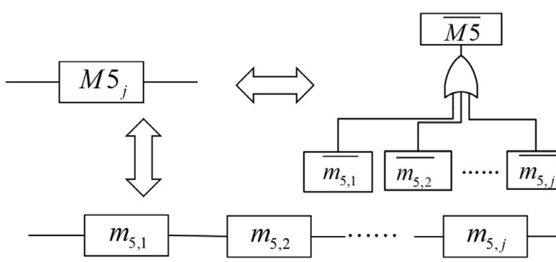

Fig. 8. The RBD and FT of the mini-components method.

Table 4
Reliability of modules 3 and 5.

	Phase 1	Phase 2	Phase 3
$R_{M_5,j}$	N/A	N/A	0.9997
$R_{M_3,j}$	N/A	0.9335	0.9079

The CDF of module 5 in phase j, $F_{M_5,j}(t)$, can be expressed as,

$$F_{M_5,j}(t) = \left[1 - \prod_{i=1}^{j-1}\left(1 - p_{M_5,i}(T_i)\right)\right] + \left[\prod_{i=1}^{j-1}\left(1 - p_{M_5,i}(T_i)\right)\right] \cdot p_{M_5,i}(t) \tag{14}$$

where T_i represents the time duration of phase i and $p_{M_5,j}(t)$ denotes the failure probability of module M_5 at time t. Time t is measured from phase j. The first term of Eq. (17) is the probability that the system fails in the first $j-1$ phases and the second term is the probability that the system fails at time t in phase j.

With the parameters shown in Table 3 and Eqs. (13) and (14), the reliability of module 5 at the end of each phase, $R_{M_5,j}(t)$, can be evaluated, and the results are shown in Table 4. Similarly, the reliability of module 3 can also be evaluated, and the results are also shown in Table 4.

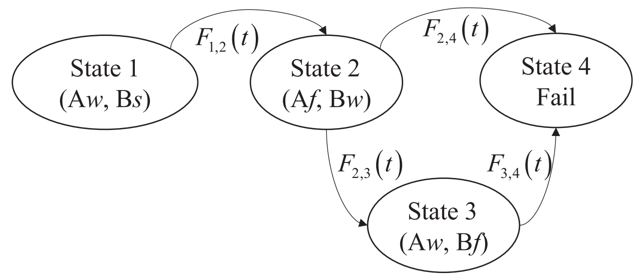

Fig. 9. The state transition diagram for module 1.

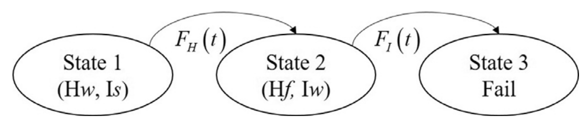

Fig. 10. The state transition diagram for module 4.

Table 5
State probabilities of module 1.

	S1	S2	S3	S4
T_1	0.9999	1.7669×10^{-4}	1.2071×10^{-10}	1.132×10^{-8}
T_2	0.9961	0.0039	1.4015×10^{-9}	3.2951×10^{-6}
T_3	0.9897	0.0102	4.008×10^{-6}	3.552×10^{-5}

Table 6
State probabilities of module 4.

	S1	S2	S3
T_1	0.9993	6.1359×10^{-4}	1.1635×10^{-7}
T_2	0.9843	0.0157	5.314×10^{-5}

5.1.2. The dynamic module without structure variation

From Fig. 6, we can see that module 1 (M1) and module 4 (M4) are dynamic modules without structure variation. In other words, the system structures of these two modules do not change in different phases. According to the dynamic behaviors of the two modules, the system state transition figures are shown as Figs. 9 and 10. The module state probabilities in one phase can be evaluated by the approximation method proposed in Section 2. To deal with the dependency across phases, the module state at the start of phase i is set to be equal to the state at the end of last phase. By this method, the state probabilities of module 1 and module 4 are evaluated and shown in Tables 5 and 6.

5.1.3. The dynamic module with structure variation

From the FT model in Fig. 6, we can see that the working components of module 2 are different in different phases. So a specially designed

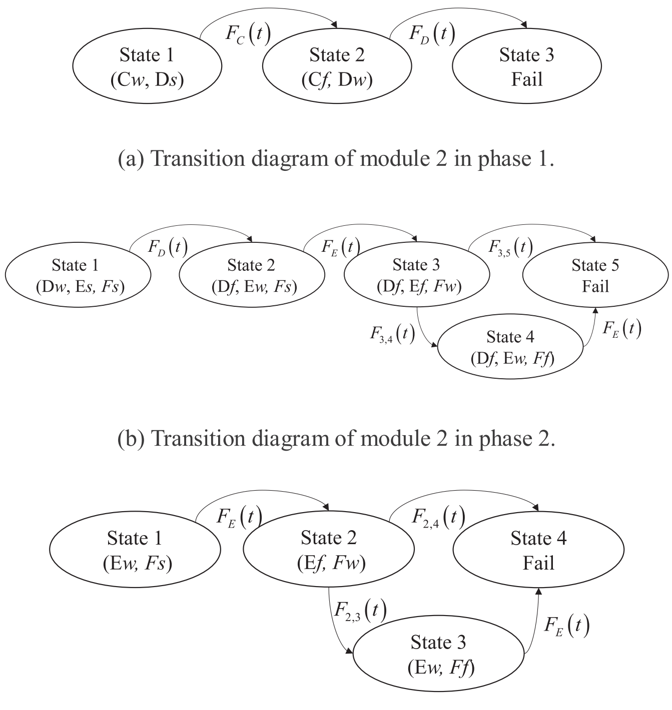

(a) Transition diagram of module 2 in phase 1.

(b) Transition diagram of module 2 in phase 2.

(c) Transition diagram of module 2 in phase 3.

Fig. 11. The state transition diagram for module 2 in three phases.

Table 7
State probabilities of module 2.

	S1	S2	S3	S4	S5
T_1	0.9993	0.0012	1.046×10^{-7}	N/A	N/A
T_2	0.9999	0.0110	3.6455×10^{-11}	3.455×10^{-11}	5.358×10^{-7}
T_3	0.9998	1.894×10^{-4}	2.2699×10^{-9}	5.401×10^{-7}	N/A

method is needed to deal with the module 2. It is important to note that, although the system structures are different in different phases, the components' states are the same between the end of one phase and the beginning of the next phase. Based on this characteristic, the module reliability can be assessed by three steps.

Step 1: Construct the state transition diagram for each phase according to its own dynamic behaviors. In this paper, the module 2 is working in all three phases and the state transition diagram for each phase is shown in Fig. 11.

Step 2: Construct the relationship between the states of every two adjacent phases according to the system structure [26]. The relationship of states between every two phases of module 2 is shown in Fig. 12. From Fig. 12, we can see that both state 1 and state 2 of phase 1 are mapped into state 1 of phase 2. The reason is that component D does not fail if module 2 stays in state 1 or state 2, and module 2 will stay in state 1 at the beginning of phase 2 if component D does not fail.

Step 3: Evaluate the module reliability by the approximation method from one phase to the next according to the relationship between every two adjacent phases and the approximation method. The module state probabilities at the end of each phase are shown in Table 7.

5.2. System reliability

In the last section, the reliability of each module has been evaluated already. With the independent basic events, the system reliability can be

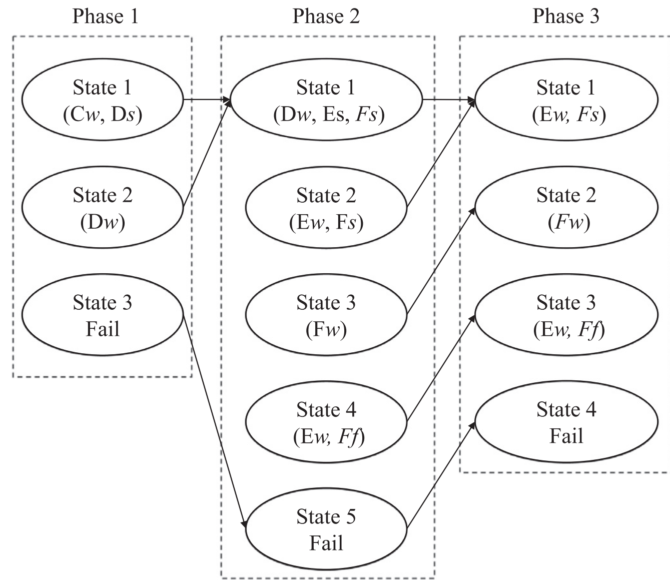

Fig. 12. The states relationship between two adjacent phases of module 2.

Table 8
Rules of phase algebra ($i<j$).

$M_i \cdot M_j \to M_j$	$\overline{M}_i + \overline{M}_j \to \overline{M}_j$
$\overline{M}_i \cdot \overline{M}_j \to \overline{M}_i$	$M_i + M_j \to M_i$
$\overline{M}_i \cdot M_j \to 0$	$\overline{M}_i + M_j \to 1$

assessed efficiently by the 5-step PMS–BDD method, proposed by Zang and Trivedi [2] and used in [1,7]. The PMS–BDD method can combine the BDD models for the phases by phase algebra shown as Table 8 to obtain the final BDD to evaluate the system unreliability. If the variables linked by edges directly belong to different variables, the evaluation method will be the same as the traditional BDD method. But if they belong to the same components in different phases, the phase algebra can be used to cancel the amount of the final BDD model.

On the other hand, the size of a BDD heavily depends on the order of variables. There exist two phase-dependent operation (PDO) ways: forward PDO and backward PDO. According to [2], the BDD generated by backward PDO (phase-dependent operation) is much smaller than that generated by the forward PDO so that the system reliability evaluation is easier. Applying the backward PDO in the AOCS and taking an order of $M_{1,3} < M_{1,2} < M_{1,1} < M_{2,3} < M_{2,2} < M_{2,2} < M_{3,3} < M_{3,2} < M_{3,1} < M_{4,2} < M_{5,3}$, each phase of the AOCS can be transferred from the FTs in Fig. 6 to the BDD models in Fig. 13.

By applying the phase algebra, the BDD models of the three phases can be combined and simplified as Fig. 14.

The system reliability R_{sys} is the probability of the SDP from the root to the vertex '0' through the system BDD figure. From Fig. 14, we can get the disjoint path: $M_{1,3}M_{2,3}M_{3,3}M_{4,2}M_{5,3}$. According to the SDP, the system reliability can be assessed by,

$$\begin{aligned} R_{sys} &= P\left(\overline{M_{1,3}M_{2,3}M_{3,3}M_{4,2}M_{5,3}}\right) \\ &= P\left(\overline{M_{1,3}}\right)P\left(\overline{M_{2,3}}\right)P\left(\overline{M_{3,3}}\right)P\left(\overline{M_{4_2}}\right)P\left(\overline{M_{5,3}}\right) \\ &= P\left(1-P\left(S4_{M1}(T_3)\right)\right)P\left(1-P\left(S4_{M2}(T_3)\right)\right)R_{M_3}(T_w) \\ &\quad P\left(1-P\left(S3_{M4}(T_1+T_2)\right)\right)R_{M_5}(T_w) \end{aligned} \tag{15}$$

where Si_{Mj} represents the state i of module j and T_w represent the whole lifetime that $T_w = T_1 + T_2 + T_3$. With Eq. (15), the system reliability of the PMS can be computed as 0.907603.

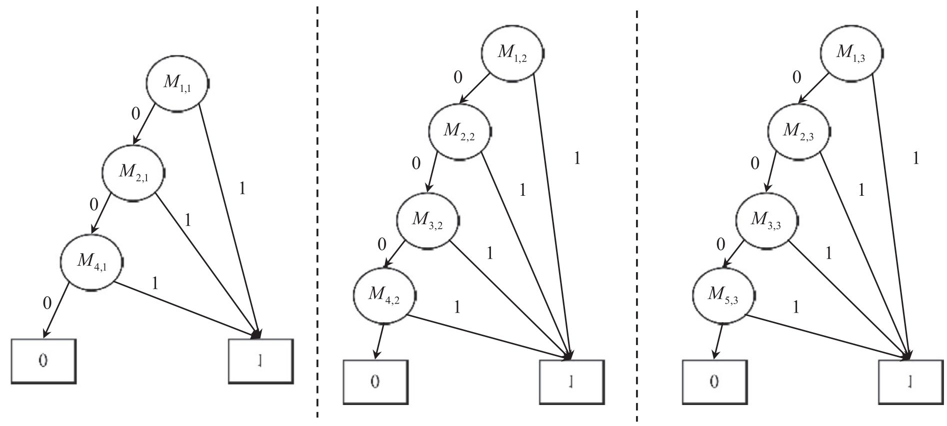

Fig. 13. The BDD models for each phase of the AOCS.

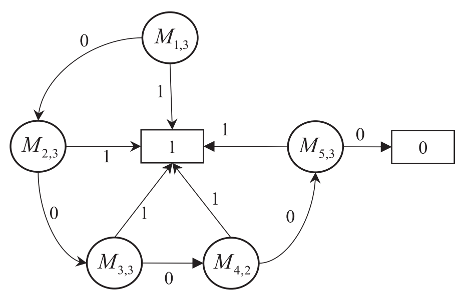

Fig. 14. The BDD model for the multi-phased AOCS.

6. Conclusions

In this paper, the reliability modelling and assessment of a realistic multi-phase system, AOCS in manmade satellite that consists of cold standby non-exponential components, is investigated. Meanwhile only part of the components can be repaired due to the weight restriction. With the non-exponential distributions, the traditional Markov process is not applicable. So the semi-Markov process is used to address this problem. To calculate the complicated integral equations in the SMP, an approximation method is proposed and the accuracy of this method is checked carefully.

In this paper, the system configuration and the working procedure of the multi-phased altitude and orbit control system (AOCS) in manmade satellite are introduced in detail. Through the modularization method, the system is divided into three types of modules: static modules, and dynamic modules with and without structure variation. The reliability of the dynamic modules can be addressed by the SMP and approximation methods. And the static modules can be solved by the mini-component method. The reliability of the multi-phased AOCS can be addressed throuth integrating the results of all the modules by the PMS-BDD model.

In this paper, we mainly focus on a multi-phased system with cold standby and partial repaired components in the AOCS of manmade satellite, but in reality a system can have much more complicated dynamic behaviors such as common-cause failures. In addition, the numbers of phases for certain systems can easily exceed three if the phase is divided precisely. Future works will be focused on these directions.

Acknowledgments

This study was sponsored by the National Natural Science Foundation of China under Grant No. 51775090 and China Scholarship Council No. 201606070066.

References

[1] Xing L, Dugan JB. Analysis of generalized phased-mission system reliability, performance, and sensitivity. IEEE Trans Reliab 2002;51(2):199–211.
[2] Zang X, Sun H, Trivedi KS. A BDD-based algorithm for reliability analysis of phased-mission systems. IEEE Trans Reliab 1999;48(1):50–60.
[3] Ou Y, Dugan JB. Modular solution of dynamic multi-phase systems. *IEEE* Trans Reliab 2004;53(4):499–508.
[4] G. Levitin, L. Xing and S.V. Amari. Recursive algorithm for reliability evaluation of non-repairable phased mission systems with binary elements. 2012, 61(2): 533–542.
[5] Xing L, Meshkatb L, Donohue SK. Reliability analysis of hierarchical computer-based systems subject to common-cause failures. Reliab Eng Syst Saf 2007;92(1):351–9.
[6] Alam M, Al-Saggaf UM. Quantitative reliability evaluation of repairable phased-mission systems using Markov approach. IEEE Trans Reliab 1986;35(1):498–503.
[7] Xing L, Amari SV. Reliability of phased-mission systems. In: Misra KB, editor. Handbook of performability engineering. Berlin, Germany: Springer; 2008. p. 349–68. ch. 23:.
[8] Peng W, Li YF, Yang YJ, et al. Leveraging degradation testing and condition monitoring for field reliability analysis with time-varying operating missions. IEEE Trans Reliab 2015;64(4):1367–82.
[9] Mi J, Li YF, Liu Y, et al. Belief universal generating function analysis of multi-state systems under epistemic uncertainty and common cause failures. IEEE Trans Reliab 2015;64(4):1300–9.
[10] Coit DW. Cold-standby redundancy optimization for nonrepairable systems. IIE Trans Reliab 2001;33(6):471–8.
[11] Levitin G, Xing L, Dai Y. Minimum mission cost cold-standby sequencing in non-repairable multi-phase systems. IEEE Trans Reliab 2014;63(1):251–8.
[12] Levitin G, Xing L, Dai Y. Minimum mission cost cold-standby sequencing in non-repairable multi-phase systems. IEEE Trans Reliab 2014;63(1):251–8.
[13] Jiang T, Liu Y. Parameter inference for non-repairable multi-state system reliability models by multi-level observation sequences. Reliab Eng Syst Saf 2017;166:3–15.
[14] Liu Y, Chen CJ. Dynamic reliability assessment for nonrepairable multistate systems by aggregating multilevel imperfect inspection data. IEEE Trans Reliab 2017.
[15] Li YF, Mi J, Liu Y, et al. Dynamic fault tree analysis based on continuous–time Bayesian networks under fuzzy numbers. Proc Inst Mech Eng Part O 2015;229(6):530–41.
[16] Mi J, Li YaYF, Peng W, Huang HZ. Reliability analysis of complex multi-state system with common cause failure based on evidential networks. Reliab Eng Syst Safe 2018;174:71–81.
[17] Huang HZ, Huang CG, Peng Z, Li YF, Yin H. Fatigue life prediction of fan blade using nominal stress method and cumulative fatigue damage theory. Int J Turbo Jet Eng 2017. doi:10.1515/tjj-2017-0015.
[18] Lisnianski A, Levitin G. Multi-state system reliability assessment, optimization and applications. Singapore: World Scientific Publishing; 2003.
[19] Lisnianski A, Frenkel I, Ding Y. Multi-state system reliability analysis and optimization for engineers and industrial managers. London: Springer; 2010.
[20] Cao Y, Sun H, Trivedi KS, et al. System availability with non-exponentially distributed outages. IEEE Trans Reliab 2002;51(2):193–8.
[21] Boehme TK, Preuss W, Van der Wall V. On a simple numerical method for computing Stieltjes integrals in reliability theory. Probab Eng Inf Sci 1991;5(1):113–28.
[22] Zio E, Librizzi M. Direct Monte Carlo simulation for the reliability assessment of a space propulsion system phased mission (PSAM-0067). In: Proceedings of the eighth international conference on probabilistic safety assessment & management (PSAM). ASME Press; 2006.
[23] Zio E, Pedroni N. Reliability estimation by advanced Monte Carlo simulation. Springer series in reliability engineering. Springer; 2012.
[24] Dutuit Y, Rauzy A. A linear-time algorithm to find modules of fault trees. IEEE Trans Reliab 1996;45(3):422–5.
[25] Huang J, Zuo MJ. Multi-state k-out-of-n system model and its applications. In: Proceedings of annual reliability and maintainability; 2010. p. 264–8.
[26] Wang C, Xing L, Peng R, et al. Competing failure analysis in phased-mission systems with multiple functional dependence groups. Reliab Eng Syst Saf 2017;164:24–33.